

Global anthropogenic heat emissions from energy consumption, 1965–2100

Yan Lu¹ · Haikun Wang¹ · Qin'geng Wang^{1,2} ·
Yanyan Zhang¹ · Yiyong Yu¹ · Yu Qian¹

Received: 22 March 2017 / Accepted: 8 October 2017 / Published online: 20 October 2017
© Springer Science+Business Media B.V. 2017

Abstract Anthropogenic heat emission (AHE) is an important contributor to regional climate change, and may affect air quality in many ways. To gain a complete picture of global AHEs and lay a basis for modeling, in this study, global and regional AHEs from energy consumption are estimated for the past nearly five decades, and projected for the future through the year 2100. From 1965 to 2013, global AHE increased from 148 to 485 EJ/year, and the anthropogenic heat flux (AHF) over land increased from 0.03 to 0.10 W/m². Meanwhile, AHE per capita increased from 44.6 to 68.1 GJ. Regional differences are remarkable. In 2013, AHFs in Asia Pacific (AP), the Middle East (ME), North America (NA), Europe and Eurasia (EE), South and Central America (SCA), and Africa (AF) were 0.23, 0.22, 0.09, 0.08, 0.04, and 0.02 W/m², respectively. During the past 50 years, AHFs in ME, AP, AF, and SCA have increased by factors of 15.3, 10.8, 5.6, and 4.0. However, growth in NA and EE has been relatively slow. In the high, moderate, and low scenarios, by 2100, the terrestrial AHFs are projected to be 0.28, 0.24, and 0.19 W/m², respectively. The largest increase would occur in Asia and ME. Although the mean AHF is small compared to the forcing of GHGs, it may exert quite distinctive effects on the climate and the environment because of the surface-based emissions and uneven geographical distribution.

Electronic supplementary material The online version of this article (<https://doi.org/10.1007/s10584-017-2092-z>) contains supplementary material, which is available to authorized users.

✉ Qin'geng Wang
wangqg@nju.edu.cn

¹ State Key Laboratory of Pollution Control and Resources Reuse, School of the Environment, Nanjing University, Nanjing 210023, China

² Jiangsu Collaborative Innovation Center of Atmospheric Environment and Equipment Technology (CICAET), Nanjing University of Information Science and Technology, Nanjing 210044, China

1 Introduction

Climate change has been recognized as an important global environmental issue, with widespread impacts on human and natural systems (IPCC 2014). Beside the emission of greenhouse gases (GHGs), many studies have suggested that anthropogenic heat emission (AHE) may play an important role in climate change, especially on city or regional scales. One of the most significant effects is reinforcing the urban heat island (UHI). Bohnenstengel et al. (2013) found that AHE in London could increase the UHI by 1 °C in May and 1.5 °C in December. Similar results have also been reported in many other cities, such as Tokyo (Kimura and Takahashi 1991), Ruhr area (Block et al. 2004), Philadelphia (Fan and Sailor 2005), Beijing (Yu et al. 2014), and Shanghai (Xie et al. 2016). Consequently, AHE was also found to have notable influences on the structure of the planetary boundary layer (Krpó et al. 2010; Miao et al. 2009; Yu et al. 2014), air quality (Ryu et al. 2013; Xie et al. 2016; Yu et al. 2014), and human health (Merbitz et al. 2012).

In view of the potential significance of AHE mentioned above, current knowledge of global AHE is far from sufficient. Most of the studies have focused on individual cities or countries, and various methods have been applied. For example, Ichinose et al. (1999) studied AHE in Tokyo using a bottom-up approach with a detailed energy consumption dataset. Ferreira et al. (2011) estimated AHE in the city of São Paulo, Brazil, using a top-down inventory method with statistical data of primary energy consumption and population. Quah and Roth (2012) calculated AHE in Singapore by combining the top-down and bottom-up approaches. Offerle et al. (2005b) estimated anthropogenic heat flux (AHF) over an area near the center of the city Lodz, Poland, by measuring the surface energy balance. Since these studies were based on different sources of data and methodologies, comparability of the results is limited, making it difficult to study climatic effects on a global scale. However, studies focusing on global AHE are relatively rare. Flanner (2009) estimated the global AHE in 2005 based on country-specific data of non-renewable energy consumption. An inventory of AHE for 2040 was projected by assuming growth rates of energy consumption for different regions of economic classification, and an inventory for 2100 was derived assuming a uniform growth rate (2% per year) after 2040. Allen et al. (2011) developed a model of large-scale urban consumption of energy, in which specific diurnal and seasonal variations can be considered. The model was used to simulate AHF from the global scale to individual cities in 2005, and showed that the urban AHF averaged globally had a diurnal range of 0.7–3.6 W/m².

Although past studies have presented plenty of information about the global AHE, there are two questions that need to be answered in depth. Firstly, as the main sources of anthropogenic heat, energy consumption has increased from 157 to 533 EJ/year from 1965 to 2013 (BP 2014), which implies that global AHE has also grown so much and could cause more noteworthy effects on climate and atmospheric environment than before. However, little information has been reported on how and how much the AHE has evolved in both spatial and temporal dimensions during the past decades. Second, with the fast development of the world economy and technologies, energy consumption will be still facing great changes in the future, not only in quantitative and structural terms, but also in temporal and spatial patterns of distribution over the world. Therefore, it makes great sense to study the corresponding variation trends in AHE basing on related projections on energy consumption in the future.

This study aims to describe a comprehensive picture of the global AHE by energy consumption. Current status and spatio-temporal evolutions from 1965 to 2013 are presented. Future trends until 2100 are projected based on scenario analysis. Some implications on

climate change are discussed. In addition, by providing an inventory with fine resolution and new data, this study lays a good ground-work for modeling studies of global climate and the environment.

2 Methodology and data

2.1 Methodology

In this work, the top-down energy inventory approach was used as an essential method to estimate the AHE, which requires data on large aggregate scales in order to downscale to smaller scales of interest (Lee et al. 2009). Global AHE from energy consumption was estimated at the country level, covering a total of 67 countries listed in the BP Statistical Review of World Energy (BP 2014). In countries where country-based data were not available, the AHEs were estimated based on continent-level data, also listed in the BP statistics, which account for about 4.0% of the global total energy consumption. As suggested by Flanner (2009), renewable energy, such as wind power and hydropower, does not constitute a new source of heat to the global climate system, serving more as a redistributor in the energy budget. Therefore, AHE from renewable energy consumption is excluded when focusing on AHE on a global or regional scale in this study.

The difference between the reported time of energy consumption and the real time of heat emission was ignored in this study. In addition, it is difficult to specify the efficiency of energy conversion to heat because of the complexity of energy conversion processes (Lee et al. 2009). For simplicity, all energy consumption is assumed to eventually dissipate into the Earth's atmosphere in the form of heat. When focusing on the ensemble features of the AHE, uncertainties induced by the above assumption should be small.

Population is chosen as a surrogate to redistribute the AHEs within a country to obtain a gridded inventory with finer spatial resolution, since exact geographical distribution of energy consumption is often unavailable. On a large scale, the population can well reflect the intensity of human's activity, and data are readily available from the United Nations Population Division and Columbia University's Socioeconomic Data and Applications Center. ArcGIS (version 10.2) is applied to process and analyze the relevant data.

In order to know the possible AHE in the future, three scenarios are defined in this study. The scenarios were characterized as high, moderate, and low, according to energy consumption from RCP8.5, RCP4.5, and RCP2.6 in the IPCC Fifth Assessment Report (IPCC 2014). The world is classified into eight regions as specified in the World Energy Outlook 2014 (IEA 2014), with three OECD and five non-OECD regions. The OECD regions include the Americas, Europe, and Asia–Oceania, and the non-OECD regions include Eastern Europe/Eurasia, Asia, the Middle East, Africa, and Latin America.

2.2 Data sources

Energy consumption data from 1965 to 2013 and the energy value of each type of fossil fuel were collected from the BP Statistical Review of World Energy (BP 2014), which provides objective and globally consistent data on energy production and consumption. As mentioned above, in order to obtain a gridded inventory with finer resolution, population is chosen as a surrogate to redistribute the AHEs within a country. The database of global population density

(with a resolution of $2.5' \times 2.5'$), which was obtained from Columbia University's Socioeconomic Data and Applications Center (<http://sedac.ciesin.columbia.edu/>), was applied in this study.

A number of institutions periodically publish their research on the current status and future trends in world energy consumption. In this study, global future energy consumption is taken from the IPCC emission scenarios (IPCC 2014). The detailed energy use adopted by IPCC (2014) for RCP8.5, RCP4.5, and RCP2.6 is described by Riahi et al. (2011), Thomson et al. (2011), and van Vuuren et al. (2011). The forecasts for regions were taken from the World Energy Outlook 2014 (IEA 2014), and the World Energy Scenarios: Composing energy futures to 2050 (WEC 2013). The growth rates of energy consumption in different regions and periods for the three scenarios were determined based on carefully reviewing, comparing, and integrating related data in these literatures. A summary of energy consumption for different scenarios is listed in Table 1. More detailed information about scenario settings are presented in Table S1–S3 in the online supplementary materials.

3 Results and discussion

3.1 Global and regional AHEs and AHFs from 1965 to 2013

With the increase in energy consumption, the global AHE shows a trend of sustained growth in the past five decades, with an annually averaged growth rate of approximately 2%, even though it decreased slightly in 1980–1982 and 2009 because of the world economic crisis. From 1965 to 2013, the global AHE increased from 148 to 485 EJ/year, corresponding to a mean flux over land increasing from 0.03 to 0.10 W/m². Meanwhile, the global AHE per capita increased from 44.6 to 68.1 GJ. When averaged over the whole Earth's surface, the flux increased from 0.009 to 0.030 W/m², with a value of 0.026 W/m² in 2005, which is comparable to that (0.028 W/m²) indicated by Flanner (2009). In the past five decades, the world has experienced significant changes in the structure of energy consumption, and so does in the composition of AHE. From 1965 to 2013, the proportion of AHE from oil and coal declined from 40.4 to 32.9% and from 38.1 to 30.1%, respectively. But the proportions of gas and nuclear grew greatly, from 15.8 to 23.7% and from 0.15 to 4.4%, respectively. However,

Table 1 Energy consumption (EJ/year) in the high, moderate, and low scenarios

Scenarios	Region	2020				2050				2100			
		Oil	Gas	Coal	Nuclear	Oil	Gas	Coal	Nuclear	Oil	Gas	Coal	Nuclear
High	OECD	87	65	42	22	90	95	42	31	96	127	42	37
	Non-OECD	109	78	138	7	147	166	165	25	308	268	385	97
	World	196	143	180	29	237	261	207	56	404	395	427	134
Moderate	OECD	87	64	42	21	90	91	40	28	92	118	39	32
	Non-OECD	109	77	138	7	145	146	165	22	287	222	328	42
	World	196	141	180	28	235	237	205	50	379	340	367	74
Low	OECD	87	63	42	20	88	72	40	27	89	83	37	29
	Non-OECD	108	73	137	6	137	106	158	19	209	200	236	37
	World	195	136	179	26	225	178	198	46	298	283	273	66

the AHE from global nuclear energy consumption has declined since 2011, possibly because of the Fukushima nuclear power plant accident. Anyway, emissions from fossil fuels are still high, accounting for more than 90% of the total AHE from energy consumption.

Regional variations are remarkable. Figure 1 shows the averaged terrestrial AHFs from 1965 to 2013 in North America (NA), Europe and Eurasia (EE), Asia Pacific (AP), South and Central America (SCA), the Middle East (ME), and Africa (AF). The AHFs in ME, AP, AF, and SCA have experienced very rapid growth over the past five decades, multiplied by factors of 16.3, 11.8, 6.6, and 5.0, respectively. In terms of characteristics of temporal variations in the AHFs, the six regions can be classified into three groups. Group one includes NA and EE, where the economic, technological, and social development is advanced while the economic growth is slow. In both regions, AHFs increased relatively quickly and remained the highest until 1990, but was later surpassed by AP and ME, and the changes with the year became small. Group 2 includes AP and ME, with most countries under fast industrialization. The two regions experienced very rapid growth in AHFs, from 0.02 and 0.01 W/m^2 in 1965 to 0.23 and 0.22 W/m^2 in 2013, respectively, and the fluxes have remained by far the highest since the 1990s. Group 3 includes SCA and AF, with sparse population and underdeveloped economy. AHFs in the two regions have been undergoing continuous and stable growth, from 0.008 and 0.003 W/m^2 in 1965 to 0.04 and 0.02 W/m^2 in 2013, but remained the lowest among all regions. It should be noted that AHFs in AP and ME are still growing fast away from the group 1 and group 3 regions. Regarding the AHE per capita in 2013, ME and NA were the top two regions with 252.6 and 226.8 GJ, respectively, followed by EE and AF, with 136.0 and 91.5 GJ, and the lowest two regions were AP and SCA, with 53.9 and 54.0 GJ. However, growths in AP and ME were much faster than other regions. In particular, from 1965 to 2013, AHE per capita in AP increased more than four times, while NA increased less than 4%.

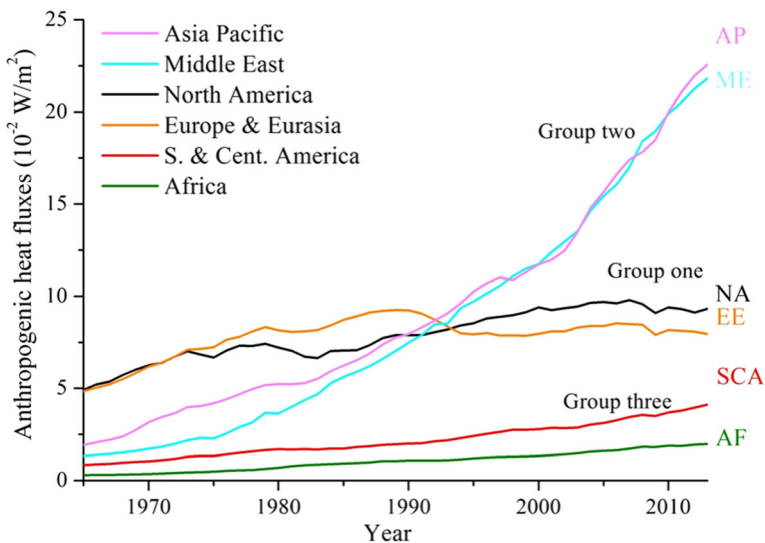


Fig. 1 Terrestrial AHFs in different regions in 1965–2013 (Group one: NA and EE; Group two: AP and ME; Group three: SCA and AF)

3.2 Gridded distribution of global AHFs and comparisons for cities

For the purpose of obtaining a finer picture of the spatial distribution of global AHF and to facilitate modeling studies of the global climate and environment, gridded distributions with a grid resolution of $0.5^\circ \times 0.5^\circ$ were constructed. As mentioned in Sect. 2, this was done essentially by reallocating the country-level estimation according to the population distribution within a country. In order to illustrate the temporal trend in global AHF, gridded distributions for 1965, 1978, 2000, and 2013 are given in Fig. 2.

It is clearly shown that AHFs are very unevenly distributed across the world. In the 1960s, Europe was obviously an area of overwhelmingly intensive AHF. Subsequently, AHFs in Asia, NA, and ME have been growing fast. By 2013, areas with intensive AHF were much more widely spread than five decades ago. Higher fluxes, above 60 W/m^2 , can be seen in Asia (Eastern China, Japan, Korea, Thailand, and India), Europe (western Russia and most of the other countries), ME (Iran and Saudi Arabia), the eastern USA, and some places in South America and AF.

Big cities are usually the places with the most intensive AHF due to huge energy consumption and dense populations. That is why most previous studies have focused on urban areas. Unfortunately, the extraordinary intensity of fluxes in cities cannot be illuminated clearly in the global picture of Fig. 2. To make up for this limitation, the AHFs in 1965, 1978, 2000, and 2013 in some typical cities, as well as related results of previous studies, are listed in Table 2. As shown in Table 2, it is difficult to obtain strict comparisons between the results of this study and previous city-oriented studies because of different methodologies, spatial scales, and data sources. However, the results agree well with one another for most cities. Generally, results based on the bottom-up inventory approach are higher, and those based on the top-down approach (as used in this study) are lower.

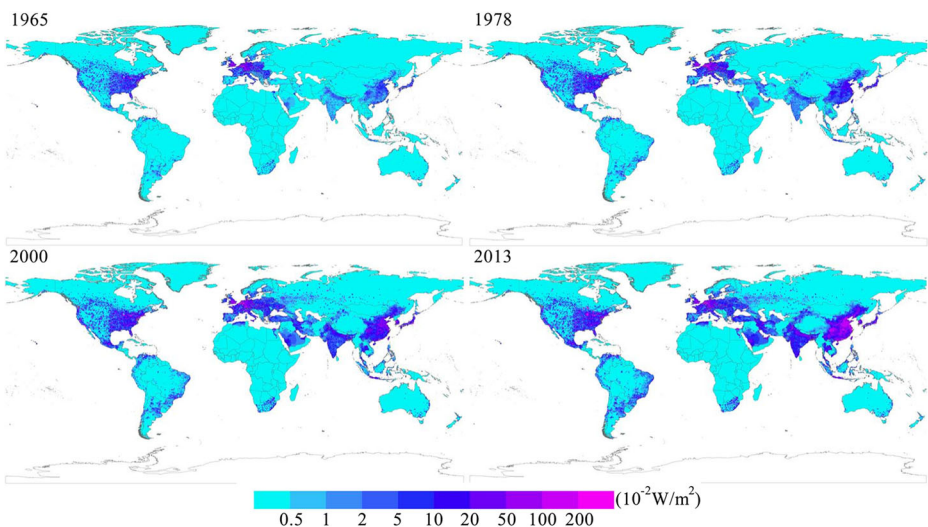


Fig. 2 Gridded distribution of global AHFs in 1965, 1978, 2000, and 2013

Table 2 Comparison of mean AHFs in different regions

Regions	AHFs (W m^{-2}) in this study ^a				Previous studies related		
	1965	1978	2000	2013	AHFs (W m^{-2})	Approach used	Reference
New York, USA	40.0	57.4	71.6	70.1	48 in 2005	Top-down	Flanner (2009)
US cities ^b	7~14	10~21	12~27	12~26	30~75 in 2000	Bottom-up, top-down	Sailor and Lu (2004)
London, UK	7.9	8.5	9.0	8.1	10.9 in 2005–20–08	Bottom-up	Iamarino et al. (2012)
Manchester, UK	4.5	4.8	5.1	4.6	6.12 in 2004	Bottom-up	Smith et al. (2009)
Tokyo, Japan	4.1	9.3	13.6	12.5	8.1 in 2005	Top-down	Flanner (2009)
Osaka, Japan	7.7	17.6	25.7	23.5	26 in 1970–19–74	Bottom-up	Ojima and Moriyama (1982)
Lodz, Poland	2.8	5.1	3.8	4.2	–3~32 in 2001~02	Energy balance	Offerle et al. (2005a)
Toulouse, France	3.3	5.5	7.2	7.1	<5~100 in 2004–05	Bottom-up, energy balance	Pigeon et al. (2007)
Gyeong-In region, Korea	0.7~1.0	2.6~3.8	13.7~20.1	19.5~28.6	28–55 in 2002	Top-down	Lee et al. (2009)
Singapore	1.5	3.4	14.0	28.1	11–85 in 2008~09	Bottom-up, top-down	Quah and Roth (2012)
Global terrestrial	0.030	0.051	0.074	0.10	0.13 in 2013	Top-down	Dong et al. (2017)
Global	0.009	0.016	0.022	0.030	0.028 in 2005	Top-down	Flanner (2009)

^a AHF here is annual mean flux

^b Chicago, Philadelphia, and San Francisco

3.3 Future trends of AHF

According to energy consumption in different regions under the three scenarios (Table 1 and Table S1–S3), and taking 2013 as the base year, global and regional AHEs and corresponding AHFs through 2100 were estimated following the same methodology as introduced in Sect. 2.1 of this paper.

Figure 3 shows variation in trends of regionally averaged terrestrial AHFs in eight regions in the high, moderate, and low scenarios. Remarkable distinctions are seen among different regions. On the whole, in 2100, fluxes in Asia, ME, and Europe are much higher than in the other five regions. Until 2050, Europe will have the most intensive AHF, about 0.47 W/m^2 , but will be gradually surpassed by Asia and ME. There are large differences between the different scenarios, especially in Asia and ME, where energy consumption in the high scenario are far larger than in the moderate and low scenarios. This implies that there are relatively large uncertainties in the development and thus in the AHF in those regions.

In the high, moderate, and low scenarios, the global total amount of AHEs by 2100 are projected to be 1360, 1160, and 920 EJ/year, respectively. Figure 4 shows the evolution trends of the terrestrial AHF in the past 50 years (1965–2013) and in the three future scenarios. It can

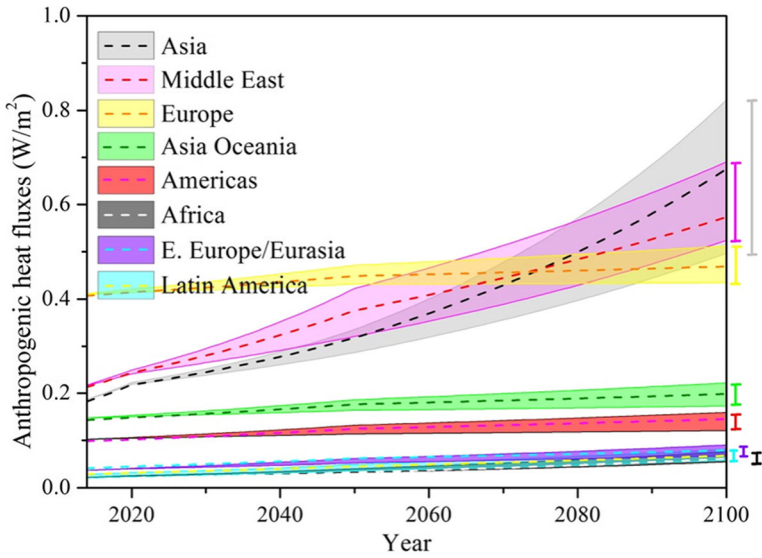


Fig. 3 Regionally averaged terrestrial AHFs in high, moderate, and low scenarios. Regions are distinguished by different colors with upper and lower boundaries representing the high and low scenarios, respectively, and with the middle dashed lines representing the moderate scenarios. Bars on the right show the ranges in 2100 between the high and low scenarios

be seen that the terrestrial mean AHFs would keep increasing for all the scenarios through the forecasted period, and even beyond. For the high, moderate, and low scenarios, the AHF could reach 0.28, 0.24, and 0.19 W/m² by 2100, respectively, corresponding to 3.3, 5.3, and 7.3% of the total forcing of the RCP8.5, RCP4.5, and RCP2.6 scenarios. However, it should be noted that the forcing effects of AHF on climate may be quite different from that of GHGs, since the

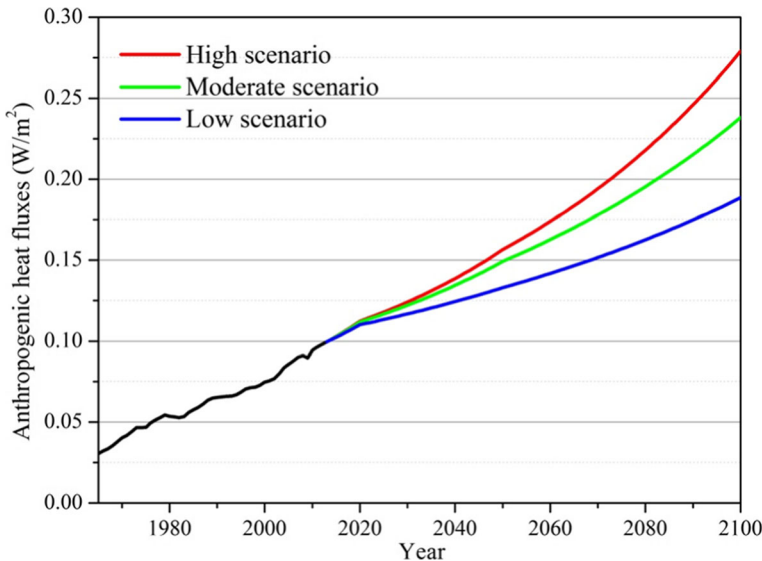


Fig. 4 Globally averaged terrestrial AHFs during the past and in the three scenarios

former heats the atmosphere directly from the surface, and with significant spatial and temporal variations.

4 Conclusions

Global AHE over 1965–2100 was estimated based on a top-down energy inventory approach and up-to-date data. From 1965 to 2013, the total amount of global AHEs from energy consumption increased from 148 to 485 EJ/year, corresponding to a mean flux over land increasing from 0.03 to 0.10 W/m². Meanwhile, global AHE per capita increased from 44.6 to 68.1 GJ. Regional variations are remarkable in both AHE and AHF. In 2013, AHFs in AP, ME, NA, EE, SCA, and AF were 0.23, 0.22, 0.09, 0.08, 0.04, and 0.02 W/m², respectively. During the past 50 years, the AHFs in ME, AP, AF, and SCA increased by factors of 15.3, 10.8, 5.6, and 4.0, respectively. However, growth in NA and EE has been relatively slow. Higher AHFs are generally located in Asia, Europe, ME, the eastern USA, and some places in South America and AF.

By 2100, in the high, moderate, and low scenarios, the global AHEs are projected to be 1360, 1160, and 920 EJ/year, corresponding to terrestrial AHFs of 0.28, 0.24, and 0.19 W/m². And the AHFs in Asia, ME, and Europe would be much higher than in the other regions. Europe would remain the most intensive until 2050, but later gradually surpassed by Asia and ME. In the future, global AHEs would shift from the Americas and Europe towards Asia, and most of the growth would come from the non-OECD countries.

Although the globally averaged AHF is small in magnitude compared to that of GHGs, attention should be paid to the distinct effects of surface-based heating, significant spatial and temporal variations, and long-lasting growth trend. This implies that in the long run, the AHE may play an important role in climate as well as the environmental system, and thus further studies are needed, and appropriate human intervention should be considered in some policymakings.

Funding This work was supported by the National Key Basic Research Program of China (2014CB441203), the National Key Research and Development Program of China (2016YFC0208504), and the National Nature Science Foundation of China (41175129).

References

- Allen L, Lindberg F, Grimmond CSB (2011) Global to city scale urban anthropogenic heat flux: model and variability. *Int J Climatol* 31:1990–2005. <https://doi.org/10.1002/joc.2210>
- Block A, Keuler K, Schaller E (2004) Impacts of anthropogenic heat on regional climate patterns. *Geophys Res Lett* 31. <https://doi.org/10.1029/2004gl019852>
- Bohnenstengel SI, Hamilton I, Davies M, Belcher SE (2013) Impact of anthropogenic heat emissions on London's temperatures. *Q J R Meteorol Soc* 140:687–698. <https://doi.org/10.1002/qj.2144>
- BP (2014) BP statistical review of world energy
- Dong Y, Varquez ACG, Kanda M (2017) Global anthropogenic heat flux database with high spatial resolution. *Atmos Environ* 150:276–294. <https://doi.org/10.1016/j.atmosenv.2016.11.040>
- Fan H, Sailor D (2005) Modeling the impacts of anthropogenic heating on the urban climate of Philadelphia: a comparison of implementations in two PBL schemes. *Atmos Environ* 39:73–84. <https://doi.org/10.1016/j.atmosenv.2004.09.031>

- Ferreira MJ, Oliveira AP, Soares J (2011) Anthropogenic heat in the city of São Paulo, Brazil. *Theor Appl Climatol* 104:43–56. <https://doi.org/10.1007/s00704-010-0322-7>
- Flanner MG (2009) Integrating anthropogenic heat flux with global climate models. *Geophys Res Lett* 36:1–5. <https://doi.org/10.1029/2008gl036465>
- Iamarino M, Beevers S, Grimmond CSB (2012) High-resolution (space, time) anthropogenic heat emissions: London 1970–2025. *Int J Climatol* 32:1754–1767. <https://doi.org/10.1002/joc.2390>
- Ichinose T, Shimodozono K, Hanaki K (1999) Impact of anthropogenic heat on urban climate in Tokyo. *Atmos Environ* 33:3897–3909
- IEA (2014) IEA world energy outlook. International Energy Agency, Paris
- IPCC (2014) Climate change 2014: synthesis report. Contribution of Working Groups I, II and III to the Fifth Assessment Report of the Intergovernmental Panel on Climate Change [Core Writing Team, R.K. Pachauri and L.A. Meyer (eds.)]. IPCC, Geneva, Switzerland, 151 pp
- Kimura F, Takahashi S (1991) The effects of land-use and anthropogenic heating on the surface temperature in the Tokyo metropolitan area: a numerical experiment. *Atmos Environ* 25B:155–164
- Krpo A, Salamanca F, Martilli A, Clappier A (2010) On the impact of anthropogenic heat fluxes on the urban boundary layer: a two-dimensional numerical study. *Bound-Layer Meteorol* 136:105–127. <https://doi.org/10.1007/s10546-010-9491-2>
- Lee SH, Song CK, Baik JJ, Park SU (2009) Estimation of anthropogenic heat emission in the Gyeong-In region of Korea. *Theor Appl Climatol* 96:291–303. <https://doi.org/10.1007/s00704-008-0040-6>
- Merbitz H, Buttstädt M, Michael S, Dott W, Schneider C (2012) GIS-based identification of spatial variables enhancing heat and poor air quality in urban areas. *Appl Geogr* 33:94–106. <https://doi.org/10.1016/j.apgeog.2011.06.008>
- Miao S, Chen F, LeMone MA, Tewari M, Li Q, Wang Y (2009) An observational and modeling study of characteristics of urban heat island and boundary layer structures in Beijing. *J Appl Meteorol Climatol* 48: 484–501. <https://doi.org/10.1175/2008jamc1909.1>
- Offerle B, Grimmond CSB, Fortuniak K (2005a) Heat storage and anthropogenic heat flux in relation to the energy balance of a central European city centre. *Int J Climatol* 25:1405–1419. <https://doi.org/10.1002/joc.1198>
- Offerle B, Grimmond CSB, Fortuniak K, Klysiak K, Oke TR (2005b) Temporal variations in heat fluxes over a central European city centre. *Theor Appl Climatol* 84:103–115. <https://doi.org/10.1007/s00704-005-0148-x>
- Ojima T, Moriyama M (1982) Earth surface balance changes caused by urbanisation. *Energy Build* 4:99–114
- Pigeon G, Legain D, Durand P, Masson V (2007) Anthropogenic heat release in an old European agglomeration (Toulouse, France). *Int J Climatol* 27:1969–1981. <https://doi.org/10.1002/joc.1530>
- Quah AKL, Roth M (2012) Diurnal and weekly variation of anthropogenic heat emissions in a tropical city, Singapore. *Atmos Environ* 46:92–103. <https://doi.org/10.1016/j.atmosenv.2011.10.015>
- Riahi K, Rao S, Krey V, Cho C, Chirkov V, Fischer G, Kindermann G, Nakicenovic N, Rafaj P (2011) RCP 8.5—a scenario of comparatively high greenhouse gas emissions. *Clim Chang* 109:33–57. <https://doi.org/10.1007/s10584-011-0149-y>
- Ryu Y-H, Baik J-J, Lee S-H (2013) Effects of anthropogenic heat on ozone air quality in a megacity. *Atmos Environ* 80:20–30. <https://doi.org/10.1016/j.atmosenv.2013.07.053>
- Sailor DJ, Lu L (2004) A top-down methodology for developing diurnal and seasonal anthropogenic heating profiles for urban areas. *Atmos Environ* 38:2737–2748. <https://doi.org/10.1016/j.atmosenv.2004.01.034>
- Smith C, Lindley S, Levermore G (2009) Estimating spatial and temporal patterns of urban anthropogenic heat fluxes for UK cities: the case of Manchester. *Theor Appl Climatol* 98:19–35. <https://doi.org/10.1007/s00704-008-0086-5>
- Thomson AM, Calvin KV, Smith SJ, Kyle GP, Volke A, Patel P, Delgado-Arias S, Bond-Lamberty B, Wise MA, Clarke LE, Edmonds JA (2011) RCP4.5: a pathway for stabilization of radiative forcing by 2100. *Clim Chang* 109:77–94. <https://doi.org/10.1007/s10584-011-0151-4>
- van Vuuren DP, Stehfest E, den Elzen MGJ, Kram T, van Vliet J, Deetman S, Isaac M, Klein Goldewijk K, Hof A, Mendoza Beltran A, Oostenrijk R, van Ruijven B (2011) RCP2.6: exploring the possibility to keep global mean temperature increase below 2°C. *Clim Chang* 109:95–116. <https://doi.org/10.1007/s10584-011-0152-3>
- WEC (2013) World energy-scenarios: composing energy futures to 2050. World Energy Council, London
- Xie M, Liao J, Wang T, Zhu K, Zhuang B, Han Y, Li M, Li S (2016) Modeling of the anthropogenic heat flux and its effect on regional meteorology and air quality over the Yangtze River Delta region, China. *Atmos Chem Phys* 16:6071–6089. <https://doi.org/10.5194/acp-16-6071-2016>
- Yu M, Carmichael GR, Zhu T, Cheng Y (2014) Sensitivity of predicted pollutant levels to anthropogenic heat emissions in Beijing. *Atmos Environ* 89:169–178. <https://doi.org/10.1016/j.atmosenv.2014.01.034>